TECHNICAL MEMORANDUMS

NATIONAL ADVISORY COMMITTEE FOR AERONAUTICS

No. 818

VALVE-SPRING SURGE

By Willy Marti

Federal Polytechnic Institute

Washington
March 1937

NATIONAL ADVISORY COMMITTEE FOR AERONAUTICS

TECHNICAL MEMORANDUM NO. 818

VALVE-SPRING SURGE*

By Willy Marti

On account of the high-speed motion of an injection valve there are set up oscillations in the valve spring and these impart a greater stress to the springs than would be the case if their inertia were neglected.

Since, for reasons of space and weight-saving, valve springs are more highly loaded than the other machine elements, it is essential to know the actual maximum stress of the spring. This knowledge is obtained either by determining the vibration strength of the springs after manufacture or by measuring the actual spring stress as a function of the speeds under which it is operated.

A knowledge of spring oscillation is also useful for the following reason. As the valve is opened the moving mass is accelerated by the pressure of the cam and again decelerated by the spring, the deceleration being assisted by the friction of the guide. When the valve closes the mass is first accelerated by the spring and then decelerated by the cam, and in this case the friction diminishes the accelerating action of the spring force. As a result of the spring oscillations the force of the spring is decreased for brief intervals so that there is set up a knocking at the bearing roller at lower speeds than would be the case if there were no such oscillations.

Under the condition of resonance the oscillating spring contributes to the general noise, since the natural frequencies of the springs commonly employed correspond to the range of audible tones. When the distance between the coils is small and the amplitude of the oscillations large the windings may come in contact with each other and damage the surface, for example, of polished springs, resulting in a lowered vibration strength of the spring if it is made of alloyed steel.

---

*"Ventilfederschwingungen." Thesis submitted in partial fulfillment of the requirements for the degree of Engineer in Mechanical Engineering Aeronautics, Federal Polytechnic Institute of Zurich, 1935, pp. 1-20.

A knowledge of the mechanism of spring oscillation is applicable to other elastic vibrating columns. In the fuel line of a Diesel injection system there occur, after injection, pressure fluctuations similar to those in the spring after the valve lift. The propagation of an electrical impulse in a cable having capacity and self induction follows, as we know, the same laws and corresponds to the same differential equation as the longitudinal waves of an elastic column.

TESTS ON SPRING SURGE THAT HAVE ALREADY BEEN PUBLISHED

Probably the simplest and clearest method of rendering the motion of the spring coils visible is that given by W. Weibull (reference 1). He fastened a small rod running radial to the spring axis to each turn and projected the shadows on a slit perpendicular to the rods. The light rays thus cut out described on a rotating photographic film the motion of each turn as a function of the time.

Figure 1 shows what happens when a weight strikes upon the spring which is in a vertical position. The impulse is propagated from coil to coil with a constant velocity and reflected at the ends of the springs. After the pressure wave has traveled several times up and down the weight is again thrown up by the spring under tension and the spring then continues to oscillate with its natural frequency. Stroboscopic methods were employed by Swan, Savage (reference 2), and von Lehr (reference 3). One arbitrary coil, usually the center one, is marked and observed stroboscopically. The motion of the coil is controlled by the cam and the coil is illuminated for an extremely short interval in the same angular position. The lift of the coil, which appears at rest, may in this way be read as a function of the angle and of the time. The time-distance curve thus obtained is the resultant of several rotations and may easily contain errors - for example, if the position of resonance is not maintained accurately as a result of small fluctuations in the speed during the test.

Lehr describes a method whereby the center spring coil having a small strip attached to it covers and uncovers a slit parallel to the spring axis and is photographed on a rotating film. The time-distance curve of

the turn then appears as a line separating bright and dark areas.

AUTHOR'S TESTS

Time-distance curves of moving machine parts may be obtained by the well-known method of using a bridge and oscillograph. A preliminary test employing this method was made on a valve spring of a Diesel engine on a test stand. To the center coil was soldered a spring steel tongue which slid along a nickel-chromium wire (fig. 2). The bridge current is proportional to the distance moved by the coil, provided the variation in the resistance is small compared to the resistance R. As may be seen by comparing an oscillogram (fig. 3) with those obtained later, the spring surge dies down very rapidly. This is due to the damping action of the strong pressure between the bridge wire and the sliding contact. A decrease in this pressure produces an unsteady fluctuation of the contact resistance and results in a deformation of the curves so that they are hardly recognizable. For this reason resonance phenomena could not be recorded although these appeared when there was no contact friction. There were nevertheless revealed speed ranges within which the amplitudes were large and others with smaller amplitudes.

In order to be able to continue the tests in the laboratory an apparatus was constructed of the form shown in figure 4, consisting of shaft, cam, roller, and spring. Two heavy pulleys at each end of the shaft acted as flywheels to render the speed uniform.

The tension produced by the vibration is largest at the spring ends. Experience has shown that spring failures occur mostly in the outermost coil unless there is some flaw in the material at some other point. Considerations of strength and acceleration forces make it advisable to investigate the stress at a spring end and not just any arbitrary deformation or velocity.

Measurement of the spring pressure with carbon plate indicators failed on account of the hysteresis effect. (The calibration curve for rising pressure does not agree with that for falling pressure.)

The compression of the last turn is a measure of the stress at the spring end but it appeared too difficult to convert this compression into a mirror rotation or electric current.

The most promising method appeared to be that of recording the change in inclination of the wire axis. To the outside turn was soldered a small knob and on it was fixed the small oscillograph mirror. The test apparatus with the spring in horizontal position was then set up near the oscillograph in such a manner that the small mirror lay in the position of the measuring loop. The reflected light ray described on the film drum the tension of the spring end as a function of the time.

Figure 5 shows oscillograms obtained by this method. Resonance is set up, as we know, when the natural frequency (or an integral multiple thereof) coincides with an integral multiple of the cam speed. For any intermediate speed the amplitude remains small. The critical speeds lie so near each other, however, that it seems practically hopeless to determine the resonance speeds in advance to a sufficient degree of accuracy so as not to have the speed of the machine coincide with any critical speed.

It may nevertheless be seen from the oscillograms (fig. 5) that the increase in the dynamic tension is not equally large for each resonance condition and this justifies the hope that it may be possible to avoid excessively large dynamic stresses within certain speed ranges.

The test method just described likewise had to be given up as not being sufficiently accurate. The testing of the spring on a spring scale showed that the relation between the stress and the light beam displacement was not linear, since the last turn lifts less and less as it is compressed. There arise, moreover, other disturbing effects due to the oscillation of the spring at right angles to the spring axis, and the resulting deformations are likewise recorded on the film and falsify the record (fig. 5, 18 to 20 oscillations per rotation).

The author had, meanwhile, for the purpose of general investigations on the Diesel engines, constructed a system of three quartz indicators whereby three different pressures could be synchronized and simultaneously recorded on a single oscillogram.

The first preliminary tests with this apparatus of Kluge and Linckh (reference 4.) showed the promising possibilities of application of radio amplifiers to the field of pressure and force recording.

When pressure is applied to a crystal cut in a special way, there arise on each surface under pressure electrical charges which charge a rotating condenser K (fig. 6) to a voltage which is proportional to the pressure. An electrostatically operating amplifier must now convert this voltage into a proportional current without thereby drawing charge from the condenser. The first tube of the amplifier therefore consists of an electrometer with amber insulated leads to the grid. (The rotating condenser of 1,000 centimeters capacity was likewise insulated against the ground by means of amber.) The tube operates with an anode voltage of only six volts as this voltage lies below the ionization voltage of the residual gas in the tube so that no grid currents are set up as a result of ionization currents. A separately heated output tube is electrostatically coupled to the electrometer tube (fig. 6).

In order that the lead from the quartz to the grid may not act as an antenna and assume too large and uncontrollable a capacity with respect to earth and thus result in high insulation losses, it must be kept very short, i.e., the amplifier must be set up near the crystal. A bare copper wire about 0.5 meter connects the center electrode with the amplifier. It appeared that a static shielding screen was unnecessary and might even prove harmful since, as a result of any fluctuations of the conductor with respect to the screen, capacity and voltage fluctuations may be set up and these may falsify the pressure oscillations on the oscillogram.

The second amplifier tube is somewhat sensitive to vibrations, especially if a tube is chosen that can give a linear characteristic with a ±5 mA current. The metal housing of the amplifier was therefore supported on weak springs and in this way the vibrations could be entirely kept down.

In practical operation larger distances between amplifier and oscillograph are unavoidable. In order to be able to use the amplifier simultaneously for observation on a ground-glass plate, a central switch desk was lowered on the oscillograph table and was connected with plug sockets and a 9-wire cable to the three amplifiers. In the diagrams (fig. 6) are shown the three amplifiers above and the switch desk below. The vertical lines to the right represent the 9-wire connecting cable to which one to three amplifiers can be connected.

Before any measurements are made the amplifier is adjusted so as to give linear readings. From the switch desk are drawn together all the relays R which connect all the grids with the potentiometer P_1. With the potentiometer equal voltage intervals can be measured and thus in a few seconds the voltage sensitivity and linearity may be checked. If necessary, the closed circuit current compensator G may be so adjusted that the linear portion of the amplifier characteristic includes the entire oscillogram width of 120 millimeters.

If the relays are again disconnected the light beam indicator remains for some time in the same position; i.e., the condenser remains charged for some time with the potential it finally received. Due to poor insulation, it discharges within a few minutes. Periodic pressure curves are therefore shifted in the direction of the oscillogram width until the mean pressure with respect to time coincides with the zero point of the condenser. The zero point of the oscillogram must be adjusted according to the form of the curve. For this purpose the potential of all the cathodes may be varied by means of the potentiometer P_2 which, however, shifts the zero points of all three curves simultaneously. To adjust the zero point of any one curve it is necessary to connect an adjustable voltage ahead of the grid between condenser and ground.

Before the oscillogram loop is connected in, the protective resistances S are disconnected in steps so that the measuring coil of the oscillogram may not be overloaded by an inaccurately compensated compensating current.

The source of current for the anode was a battery of storage cells supplying 150 volts. It is also possible to use a network connection provided the current is sufficiently well smoothed out by filters. If more current is suddenly drawn from the network the current cannot immediately adjust itself to a steady condition due to the choking action of the filter. The current must therefore be stabilized by means of a sufficiently large condenser.

THEORY OF WAVES IN VALVE SPRINGS

In the derivations given below, the following notation will be used:

d is the mean diameter of turn

J, polar moment of inertia

F, cross-sectional area of spring wire

δ, diameter of round spring wire

p, number of active spring turns

l, length of spring uncoiled

μ, reduced mass of spring per centimeter wire length $= \left(F + 4\frac{J}{d^2}\right)\frac{\gamma}{g} \cong F\frac{\gamma}{g}$

k, damping constant per centimeter of wire length

t, time variable

y, lift of a spring coil at distance x

x, distance from the fixed end of the spring

γ, specific weight of spring

g, acceleration of gravity

G, torsional modulus of spring steel

v, velocity of spring coil

τ, tension of spring

τ_o, spring tension at lift h_o

M, torsional moment corresponding to τ

h, valve lift as function of cam angle

h_o, maximum valve lift

T_o, time interval for a disturbance to run up and down the spring

w_s, speed of propagation of an elastic disturbance along the wire axis

ω, angular velocity of cam

φ, angular setting of cam

ω_o, natural angular velocity of spring

The well-known differential equation for the elastic disturbance of a spiral spring reads (reference 5):

$$\mu \frac{\partial^2 y}{\partial t^2} + k \frac{\partial y}{\partial t} = c \frac{\partial^2 y}{\partial x^2}; \qquad c = \frac{4J}{d^2} G \tag{1}$$

The velocity with which an elastic disturbance without damping is propagated along the spring wire is:

$$w_s = \sqrt{\frac{c}{\mu}} = 2\sqrt{\frac{J/d^2}{F + \frac{4J}{d^2}} \frac{G_g}{\gamma}} \cong 2\sqrt{\frac{J}{Fd^2} \frac{G_g}{\gamma}} \tag{2}$$

It may be noted that the value of $\sqrt{\frac{G_g}{\gamma}}$ is identical with the velocity of propagation of torsional disturbances in smooth rods.

Let a spring that extends to infinity in one direction have the other end moved according to a definite law of velocity. Velocity waves will be propagated along the spring axis with the disturbance velocity. Together with the velocity wave and unseparably connected with it, there is propagated a corresponding stress distribution (torsional stress).

The following application of the principle of conservation of momentum shows how the velocity and stress depend on each other: In the very short interval dt, the velocity at the starting end of the spring is changed by amount Δv, for which a change in force ΔP is required. This change in velocity has moved forward in the time dt the distance w_s dt. By the principle of conservation of momentum,

$$\Delta P \, dt = \mu \, w_s \, dt \, \Delta v$$

$$\Delta P = \frac{\Delta M}{d/2} = \mu \, w_s \, \Delta v$$

Substituting the values for μ and w_s there is obtained an expression for the dynamical torsional moment

$$\Delta M_{dyn} = \sqrt{JF \, \frac{G\gamma}{g}} \, \Delta v \qquad (3)$$

The dynamical stress becomes for all cross sections

$$\tau_{dyn} = \beta \sqrt{\frac{G\gamma}{g}} \, \Delta v \qquad (3a)$$

where the nondimensional numerical coefficient β depends only on the form of the cross-sectional area.

For steel springs with round wire section

$$\Delta\tau = 360 \, \Delta v \quad \text{approximately} \ (kg/cm^2; \ m/s)$$

In a gun spring, for example, the initial stress depends not on the spring dimensions but on the initial velocity at one end of the rebounding gun barrel, on the form of cross-sectional area of the wire, and on the material.

REFLECTION OF THE WAVES AT ENDS OF VALVE SPRING

For a spring of finite length, proportionality likewise obtains between the disturbing velocity change and the stress wave. The total stress at any point of the spring consists, however, of the superposition of all the stress waves traveling up and back.

The reflection of a disturbance, consisting of the velocity and stress waves, at a fixed wall occurs in the following manner (fig. 7):

The condition of a fixed wall requires that the velocity of the spring elements adjacent to the wall should be zero at every instant. This condition may be satisfied by superposing a moving symmetrical disturbance, as would be obtained by mirror reflection, on the original disturbance.

(In fig. 7 the velocity waves are drawn symmetrical about a point (central symmetry), since the velocities when considered as scalars have reversed signs. The velocity vectors are naturally also symmetrical about a line.)

On account of the central symmetry the velocity vanishes at the wall at each instant. The wave on the left travels to the right and is not considered for any further investigation. The wave on the right travels toward the left, is similarly reflected at the disturbing end of the spring, and so travels up and down several times.

The same phenomenon will occur when the other end of the spring is simultaneously disturbed. Both disturbances would give rise to symmetrical waves of stress which would be doubled at the wall d.

Figure 7 shows the wave drawn shorter than the length of the spring. Only two waves are therefore superposed. Actually the disturbance producing the waves is very slow compared to the velocity of propagation of the disturbance. The valve opening time is very large compared with the period T_o that it takes a wave to run up and down the spring. This fact does not in any way affect the process of reflection but makes the superposition somewhat more complicated.

The wave reflected at the fixed wall will now again be reflected at the disturbed spring end and after an interval again arrive at the fixed wall. At the wall the doubled stress waves add up after the interval T_o, the wave twice reflected after an interval $2T_o$, the wave three times reflected after an interval $3T_o$, etc.

THE DYNAMICAL STRESS OF THE VALVE SPRING FOR A SINGLE LIFT OF THE VALVE

From the discussion given above, the dynamic stress at the fixed end of the spring is the resultant of the stress waves reaching that end after equal intervals (after each period T_o), the stress doubling at each reflection. If we denote the disturbing velocity function by v_t, then the total torsional moment at the fixed wall for a single valve lift and for springs of any cross section is according to equation (3):

$$M_{dyn} = \sqrt{JF\frac{G\gamma}{g}}\,(2v_t + 2v_{t-T_o} + 2v_{t-2T_o} + 2v_{t-3T_o} \cdots\cdots)$$

In order to obtain the simplest possible relations, this equation will be converted into nondimensional form. Since the cam angle φ equals ωt, the foregoing equation may be written with indices φ, $\varphi - \omega T_o$, $\varphi - 2\omega T_o$, $\varphi - 3\omega T_o$, $\varphi - 4\omega T_o$, etc.

Let the movable end of the spring move with lift h, which is a function of φ. The velocity is then

$$v_\varphi = \omega \frac{dh}{d\varphi}$$

and the above equation is transformed into

$$M_{dyn} = \sqrt{JF\frac{G\gamma}{g}}\,\omega\left[2\left(\frac{dh}{d\varphi}\right)_\varphi + 2\left(\frac{dh}{d\varphi}\right)_{\varphi-\omega T_o} + 2\left(\frac{dh}{d\varphi}\right)_{\varphi-2\omega T_o} \cdots\cdots\right] \qquad (4)$$

For a slow compression of the spring the torsional moment of the spring according to the theory of strength of materials is

$$M = \frac{2JG}{ld} h_o \qquad (5)$$

The difference in torsional stress between lower and upper cam positions is therefore:

$$M_o = \frac{2JG}{ld} h \qquad (6)$$

The period of a vibration, which is also the time required for a wave to run along the spring up and back, is

$$T_o = \frac{2l}{w_s} = l\sqrt{\frac{Fd^2}{J}\frac{\gamma}{G_g}}$$

and the angular frequency of the fundamental vibration is

$$\omega_o = \frac{2\pi}{T_o} = \frac{2\pi}{l}\sqrt{\frac{J}{Fd^2}\frac{G_g}{\gamma}} = \frac{2JG}{ld}\pi\sqrt{\frac{g}{JFG\gamma}} \qquad (7)$$

By combining equations (6) and (7)

$$M_o = \frac{h_o \omega_o}{\pi} \sqrt{JF \frac{G\gamma}{g}} \qquad (8)$$

Dividing equation (4) by equation (8)

$$\frac{M_{dyn}}{M_o} = \frac{\tau_{dyn}}{\tau_o} = \pi \frac{1}{h_o} \frac{\omega}{\omega_o} \left[2 \left(\frac{dh}{d\varphi}\right)_{\varphi} + \right.$$

$$\left. + 2 \left(\frac{dh}{d\varphi}\right)_{\varphi - \omega T_o} + 2 \left(\frac{dh}{d\varphi}\right)_{\varphi - 2\omega T_o} + \ldots . \right]$$

The ratio $\omega_o/\omega = z$, which is the number of natural vibrations per cam revolution, will be taken as a measure of the time. We furthermore set

$$\omega T_o = \frac{2\pi}{z}$$

so that we obtain:

$$\frac{\tau_{dyn}}{\tau_o} = \frac{\pi}{h_o z} \left[2 \left(\frac{dh}{d\varphi}\right)_{\varphi} + 2 \left(\frac{dh}{d\varphi}\right)_{\varphi - \frac{2\pi}{z}} + 2 \left(\frac{dh}{d\varphi}\right)_{\varphi - 2\frac{2\pi}{z}} + \ldots . \right] \qquad (9)$$

The stress at the moving end of the spring will then be

$$\frac{\tau_{dyn}}{\tau_o} = \frac{\pi}{h_o z} \left[1 \left(\frac{dh}{d\varphi}\right)_{\varphi} + 2 \left(\frac{dh}{d\varphi}\right)_{\varphi - \frac{2\pi}{z}} + 2 \left(\frac{dh}{d\varphi}\right)_{\varphi - 2\frac{2\pi}{z}} + \ldots . \right] \qquad (10)$$

The first wave does not enter doubled into equation (10) since it has arisen from a velocity disturbance and not by reflection.

Both curves representing equations (9) and (10) differ from equation (5) only by the superposition of the additional dynamic stress. After a time equal to the interval of lift, functions 9 and 10 become periodic.

From the relations derived above the result follows that the magnitude of natural oscillation for a single lift of the valve depends only on the cam contour and the natural frequency of the spring. The spring material and dimensions affect only the natural spring frequency. The computation of the dynamical stress is reduced to the addition of $dh/d\varphi$ curves shifted from each other by an equal amount $2\pi/z$. Magg in 1912 derived a similar though not nondimensional formula.

MEASUREMENT OF THE $dh/d\varphi$ CURVE OF THE CAM TESTED

It is not advisable to obtain the $dh/d\varphi$ curve by graphical differentiation of a measured lift curve since, as we know, the method of graphical differentiation is very inaccurate. The velocity curve, it is true, is generally known from the cam computations from which the workshop drawing has been made, but due to faults in workmanship there are errors in using the cam pattern that may not be neglected. It was therefore attempted to carry out the differentiation experimentally on the test machine and the attempt proved successful.

To one of the flywheels (fig. 4) of 370 millimeters diameter, a strip of paper divided into millimeter divisions was glued on in the direction of the perimeter, and a permanent horseshoe magnet was mounted on it. A precision dial gage was fixed on the stand so that on turning the flywheel "feeler" of the dial gage was moved by the magnet. The center of the "feeler" was at a distance of 220 millimeters from the axis of rotation. The flywheel was now turned several times accurately ± 2.50 mm $= \pm 0.65^\circ$ (5 dial gage revolutions). With a second instrument the change in lift Δh which varied between 0 and 0.80 millimeter was determined. The measuring was repeated after the magnet was shifted each time 5 mm $= 1.55^\circ$ along the millimeter paper. The quotients $\Delta h/\Delta\varphi$ could be represented without any scattering by a smooth curve as a function of φ (fig. 8). The accuracy is equal to that of the measurement of the change in lift since the change in the angle of $\pm 0.65^\circ$ corresponded to ± 250 graduation marks, so that the error for $\Delta\varphi$ could be neglected in comparison with the errors for Δh.

The positive and negative areas of the $dh/d\varphi$ curve deviated by only about 2 percent and gave the value of the maximum lift taking the scale of the figure into account. An attempt was next made to approximate the velocity curve (shown dotted in fig. 9) by a triangular-shaped curve (fig. 9). The superposition of the triangles in accordance with equation (9) yielded a curve with sharp angles different from the corresponding oscillograms to be discussed later. If, however, the accurate curve is used, there is obtained the dotted stress curve (c in fig. 9) which is appreciably different.

SIMULTANEOUS RECORDING OF THE STRESS AT BOTH ENDS OF THE SPRING

A pair of quartz crystals was connected at each end of the spring. (In piezo-electric measurements two-quartz crystals are used, in general, so as to make the insulation of only one electrode necessary (fig. 10)). On one side of the spring the force was transmitted to the crystal through a guided coupling, since rather long springs would otherwise easily buckle. A similar guide was also provided at the moving end. The weight of the latter guide, however, necessitated its acceleration so that the accelerating force was superposed on the spring force and for this reason the guide was dispensed with.

In order to test the Magg theory for the oscillations of a spring during a single lift of the valve, the stresses at both ends of the spring were computed according to equations (9) and (10) for $z = 20$ oscillations per rotation, and the same curves were obtained with the oscillograph (figs. 11 and 12).

The oscillogram was obtained for a single lift by damping the resonance vibration of the spring through hand contact. The first lift after the spring is released behaves, as is evident from figure 12, as a single lift.

The wave character of the oscillations is clearly brought out by the computed curves together with the corresponding oscillograms. The initial rise in pressure is linear like the velocity diagram and not parabolic like the lift. The pressure rise at the stationary end occurs after a delay of half a vibration period; i.e., after the disturbance has traveled from the moving to the fixed end. Figure 13 shows the stress at each end of the spring for the condition of resonance. It may be seen that it is chiefly the first harmonic that is excited. The harmonics at the ends are shifted in phase by 180°. The natural vibrations of odd order 1, 3, 5, etc., produce pressures at both ends of the spring having a phase shift of 180°, whereas those of even order are in phase. The proof for this is found in the following test:

Instead of leading the static electrical charges of each pair of quartz crystals to each amplifier, the charges were superposed and conducted to only one amplifier. The

oscillogram thus obtained then represents the instantaneous sum or arithmetical mean of the forces at the spring ends and the even orders therefore disappear from the oscillogram. Figure 14 shows, for example, such a record for $z = 19$. Actually, the 38 vibrations per rotation recorded were of the second order. Immediately thereafter, the pressure curve at the stationary end of the spring was taken for comparison on the same figure.

If the poles of one of the crystal pairs are interchanged and the charges at both ends of the springs added, the oscillogram will show the difference in spring forces. The difference includes, however, only the odd orders. The stress during the lift is no longer shown on the oscillogram (fig. 15). Only the decreasing vibration of the first order is seen and this is built up again during the lift interval.

SPRING OSCILLATION DURING A SINGLE LIFT AS A FUNCTION OF THE SPEED

In order to test the above theory of waves propagated in springs, the dynamical stress of the spring was computed for $z = 12$ to 23 oscillations per rotation. Since one oscillation within this range lasts from 15° to 30°, the velocity curves must be added 2° apart in order to attain sufficient accuracy. The shifts $(360^\circ/z)$, that is, the amounts by which the velocity curves are shifted from each other and must be added are given in the following table:

Oscillations, rotation	z=12	13	14	15	16	17	18	19	20	21	22	23
Degree shift, exact	30	27.7	25.7	24	22.5	21.2	20	18.9	18	17.2	16.4	15.7
Degree shift, approximate	30	27.5	25.5	24	22.5	21.0	20	19	18	17.0	16.5	15.5

In order to simplify the computation, the accurate values of the shifts were rounded off to integral or half-integral values. The ordinates of the velocity curve which was drawn to large scale were then tabulated for each half degree. Table I, page 17, shows, for example, the computation procedure for $z = 20$ oscillations per rotation. The column headed $(dh/d\varphi)_{\varphi}$ repeats itself in the remaining columns each time with a shift of 18°. In the column headed $\Sigma\, dh/d\varphi$ the previous columns were added, taking into account the correct sign and finally, in the last column, they were multiplied by $180^{\circ}/h_0 z \times 2$ by which the values appeared in nondimensional form τ_{dyn}/τ_0.

It may be seen from the table that after the first lift an oscillation between $\tau_{dyn}/\tau_0 = 0.139$ and -0.116 remains behind. Actually this amounts to ± 0.125. The deviation was caused by the inequality in the velocity areas mentioned above. In the diagrams later given, the error was corrected each time.

For practical purposes the foregoing computation need only partly be carried through. To compute the spring oscillations, a knowledge of a complete oscillation period at the lower position is required.

The computed curves for $z = 12$ to 23 are shown in figure 17. For greater clearness the scales were omitted since the distance between the center line of the top and bottom stops always corresponds to $\tau_{dyn}/\tau_0 = 1$.

The same diagrams were obtained with the oscillograph and are shown together in figure 16. In order that the oscillograms may correspond to a single lift resonance was again set up as described above; the oscillation was damped and the swinging recorded. The first lift after the damping is removed corresponds to a single lift. Computations and tests were carried out for the stationary end of the spring, and they agree to a sufficient degree of accuracy.* The oscillograms confirm the method of Magg.

---

*Since the damping could not be removed suddenly and often not accurately enough between two lifts, the jags on the oscillograms are somewhat smaller.

TABLE I

	$\left(\frac{dh}{d\varphi}\right)_m$								$\Sigma\left(\frac{dh}{d\varphi}\right)$	$\frac{180^\circ}{h_o z} \times \Sigma 2\frac{dh}{d\varphi} = \frac{\tau_{dyn}}{\tau_o}$
m =	φ	φ 18	φ 36	φ 54	φ 72	φ 90	φ 108	φ 126		
deg.	% cm per deg.									
0	0								0	0
2	.46								.46	.046
4	.92								.92	.092
6	1.38								1.38	.138
8	1.85								1.85	.185
10	2.31								2.31	.231
12	2.85								2.85	.285
14	3.38								3.38	.338
16	3.85								3.85	.385
18	4.31	0							4.31	.431
20	4.92	.46							5.38	.538
22	5.38	.92							6.30	.630
24	5.92	1.38							7.30	.730
26	6.00	1.85							7.85	.785
28	5.85	2.31							8.16	.816
30	5.70	2.85							8.55	.855
32	5.38	3.38							8.76	.876
34	5.00	3.85							8.85	.885
36	4.61	4.31	0						8.92	.892
38	4.23	4.92	.46						9.61	.961
40	3.77	5.38	.92						10.07	1.007
42	3.23	5.92	1.38						10.53	1.053
44	2.77	6.00	1.85						10.62	1.062
46	2.31	5.85	2.31						10.47	1.047
48	1.77	5.70	2.85						10.32	1.032
50	1.31	5.38	3.38						10.07	1.007
52	.85	5.00	3.85						9.70	.970
54	.38	4.61	4.31	0					9.30	.930
56	0	4.23	4.92	.46					9.61	.961
58	0	3.77	5.38	.92					10.07	1.007
60	0	3.23	5.92	1.38					10.53	1.053
62	0	2.77	6.00	1.85					10.62	1.062
64	0	2.31	5.85	2.31					10.47	1.047
66	0	1.77	5.70	2.85					10.32	1.032
68	0	1.31	5.38	3.38					10.07	1.007
70	0	.85	5.00	3.85					9.70	.970

TABLE I (Cont'd.)

	$\left(\frac{dh}{d\varphi}\right)_m$								$\Sigma\left(\frac{dh}{d\varphi}\right)$	$\frac{180^\circ}{h_o z} \times \Sigma 2\frac{dh}{d\varphi} = \frac{\tau_{dyn}}{\tau_o}$
m =	φ	φ 18	φ 36	φ 54	φ 72	φ 90	φ 108	φ 126		
deg.	% cm per deg.									
72	0	0.38	4.61	4.31	0				9.30	0.930
74	0	0	4.23	4.92	.46				9.61	.961
76	0	0	3.77	5.38	.92				10.07	1.007
78	0	0	3.23	5.92	1.38				10.53	1.053
80	0	0	2.77	6.00	1.85				10.62	1.062
82	- .08	0	2.31	5.85	2.31				10.39	1.039
84	- .62	0	1.77	5.70	2.85				9.70	.970
86	-1.15	0	1.31	5.38	3.38				8.92	.892
88	-1.69	0	.85	5.00	3.85				8.01	.801
90	-2.23	0	.38	4.61	4.31	0			7.07	.707
92	-2.69	0	0	4.23	4.92	.46			6.92	.692
94	-3.23	0	0	3.77	5.38	.92			6.84	.684
96	-3.69	0	0	3.23	5.92	1.38			6.84	.684
98	-4.07	0	0	2.77	6.00	1.85			6.55	.655
100	-4.54	- .08	0	2.31	5.85	2.31			5.85	.585
102	-4.92	- .62	0	1.77	5.70	2.85			4.78	.478
104	-5.23	-1.15	0	1.31	5.38	3.38			3.69	.369
106	-5.54	-1.69	0	.85	5.00	3.85			2.47	.247
108	-5.85	-2.23	0	.38	4.61	4.31	0		1.22	.122
110	-6.00	-2.69	0	0	4.23	4.92	.46		.92	.092
112	-5.69	-3.23	0	0	3.77	5.38	.92		1.16	.116
114	-5.38	-3.69	0	0	3.23	5.92	1.38		1.46	.146
116	-4.92	-4.07	0	0	2.77	6.00	1.85		1.63	.163
118	-4.38	-4.54	- .08	0	2.31	5.85	2.31		1.47	.147
120	-3.85	-4.92	- .62	0	1.77	5.70	2.85		.93	.093
122	-3.38	-5.23	-1.15	0	1.31	5.38	3.38		.31	.031
124	-2.92	-5.54	-1.69	0	.85	5.00	3.85		- .45	- .045
126	-2.38	-5.85	-2.23	0	.38	4.61	4.31	0	-1.16	- .116
128	-1.92	-6.00	-2.69	0	0	4.23	4.92	.46	-1.00	- .100
130	-1.46	-5.69	-3.23	0	0	3.77	5.38	.92	- .31	- .031
132	-1.00	-5.38	-3.69	0	0	3.23	5.92	1.38	.45	.045
134	- .53	-4.92	-4.07	0	0	2.77	6.00	1.85	1.10	.110
136	- .08	-4.38	-4.54	- .08	0	2.31	5.85	2.31	1.39	.139
138	0	-3.85	-4.92	- .62	0	1.77	5.70	2.85	.93	.093
140	0	-3.38	-5.23	-1.15	0	1.31	5.38	3.38	.31	.031

COMPUTATION OF AMPLITUDE OF OSCILLATION FOR A SINGLE LIFT BY HARMONIC ANALYSIS

The velocity may be represented by the following Fourier series:

$$\frac{dh}{d\varphi} = \begin{cases} a_1 \sin \varphi + a_2 \sin 2\varphi + a_3 \sin 3\varphi \ldots\ldots \\ + b_1 \cos \varphi + b_2 \cos 2\varphi + b_3 \cos 3\varphi \ldots\ldots \end{cases}$$

The method of computation indicated by equations (9) and (10) may be applied to each harmonic separately since the partial results may be superposed for each harmonic.

The superposition of the first sine term according to equation (9), namely:

$$a_1 \sin \varphi + a_1 \sin \left(\varphi - \frac{2\pi}{z}\right) + a_1 \sin \left(\varphi - 2\,\frac{2\pi}{z}\right) +$$

$$+ \ldots\ldots a_1 \sin \left(\varphi - [z - 1]\,\frac{2\pi}{z}\right)$$

becomes zero as one may easily convince oneself by drawing a star-shaped vector diagram. The z vectors form angles of $2\pi/z$ with each other and balance out. The same holds for the first cosine term.

The vectors a_2 and b_2 form angles of $2 \times \frac{2\pi}{z}$ and their vector sum likewise vanishes.

It will be found, finally, that the superposition of the harmonics 1 to $z - 1$; $z + 1$ to $2z - 1$; $2z + 1$ to $3z - 1$, etc., cancel out and only the harmonics z, $2z$, $3z$, $4z$, etc., add up to give the superposition sum, namely:

$$za_z \sin 2\varphi + za_{2z} \sin 2z\varphi + za_{3z} \sin 3z\varphi + \ldots +$$

$$+ zb_z \cos 2\varphi + zb_{2z} \cos 2z\varphi + zb_{3z} \cos 3z\varphi + \ldots$$

Substituting the above in equation (9), we obtain the relation:

$$\frac{\tau_{dyn}}{\tau_o} = \frac{2\pi}{h_o} \begin{cases} a_z \sin z\varphi + a_{2z} \sin 2z\varphi + a_{3z} \sin 3z\varphi \ldots \\ +b_z \cos z\varphi + b_{2z} \cos 2z\varphi + b_{3z} \cos 3z\varphi \ldots \end{cases} \qquad (11)$$

Equation (11) expresses the condition that the natural oscillations of the spring are in resonance with the harmonics of the disturbing velocities and the coefficient of the indices denotes the number of oscillation loops. The amplitude of the forced oscillation is proportional to the exciting harmonic of the $dh/d\varphi$ curve.

In order to compare equation (11) with the previous results, the velocity curve of the test cam was developed into a Fourier series according to the method of Runge and with the aid of 72 ordinates. From the results of the example (fig. 9), it follows that a smaller number of ordinates would not be advisable. In the analysis, however, the higher ordinates may be neglected and the forced oscillation after a single lift assumed to be a sine wave to a first approximation.

The agreement between the "oscillation spectrum" obtained by each method is satisfactory (fig. 18). The addition of z curves shifted with respect to each other by $360^\circ/z$ leads to quicker results, however, than the harmonic analysis.

EFFECT OF CAM PROFILE

From equation (9), it follows that the contour of the cam determines the magnitude of the oscillation amplitudes. An example of a simplified velocity curve shows what points must be considered in order to reduce to possibilities of spring surging. Interesting information is obtained when there is first investigated the results of a single lift by the cam, (dynamic compression of an elastic column). For this investigation two velocity curves will be employed - one consisting of an isosceles triangle, and one of a half-sine wave. Instead of z oscillations per rotation, the relation $\epsilon = T'/T_0$ will be introduced, where T_0 denotes the natural period of the oscillation of the first order, and T' the interval of lift equal to the base of the triangle or of the sine half-wave. At the upper stop the spring remains in an oscillating condition. The maximum amplitudes $\Delta\tau_{max}$ are expressed as a fraction of τ_0 which is the stress corresponding to the maximum lift.

For the triangular velocity curve the peaks of the stresses are

$$\frac{\Delta\tau_{max}}{\tau_o} = \frac{4}{\epsilon}\left(0.5 + m - 2\,\frac{1 + 2 + 3 \ldots m}{\epsilon}\right) - 1 \qquad (12)$$

where for ϵ = 0 to 2, 2 to 4, 4 to 6, 6 to 8, etc.

m = 0 1 2 3

For the sine half-wave within short ranges, the following formulas hold:

$$\frac{\Delta\tau_{max}}{\tau_Q} = \frac{a\pi}{2\epsilon} - 1 \qquad (13)$$

for ϵ = 0 to 1.5 $a = 1$

1.5 to 2.5 $a = 2 \sin \pi \frac{\epsilon - 1}{2\epsilon}$

2.5 to 3.5 $a = 1 + 2 \sin \pi \frac{\epsilon - 2}{2\epsilon}$

3.5 to 4.5 $a = 2 \sin \pi \frac{\epsilon - 1}{2\epsilon} + 2 \sin \pi \frac{\epsilon - 3}{2\epsilon}$

4.5 to 5.5 $a = 1 + 2 \sin \pi \frac{\epsilon - 2}{2\epsilon} + 2 \sin \frac{\epsilon - 4}{2\epsilon}$

Both formulas are graphically given in figure 19 and were obtained in the following way: The curves were graphically superposed in accordance with equation (9). This representation served only as an approximate indication and for greater accuracy the addition was performed analytically. A special formula was thus found for each region between the tangent discontinuities in figure 19. The formulas for all the subdivisions arranged in series showed a certain regularity and from these, formulas (13) and (14) were derived.

There are, accordingly, certain ratios for T'/T_o for which no - or only slight - oscillations are brought about by the compression (zero point of the first kind). If the upper portion of the time-velocity curve of the spring end as it moves up, is symmetrical with respect to the center of the lift, and if the up and down motions are symmetrical, then the following characteristics appear: The form and amplitude of the oscillation are congruent for the up and down travel and differ by a phase shift which depends on the time interval T'' between up and

down travel. The oscillations of the two halves of the curve either add up or cancel each other according to the phase shift (zero point of the second kind). In order to illustrate this behavior, a few oscillation diagrams are shown on figure 20 for the triangular velocity curves with $T'' = 1.5\ T'$. For $z = 26.2$ and 13.1 or $T'/T_o = 4$ and 2, no oscillations are set up at the upper travel and therefore also none at the lower. For $z = 21.8$ and $z = 17.5$ there are some oscillations after the up travel but these disappear during the down travel. This case always occurs when T'' is an integral multiple of the natural vibration period T_o.

The greatest amplitude within the range investigated occurs at $z = 19.6$ where the phase difference is such that the amplitude is doubled. The triangular velocity curve investigated coincides approximately with the curve of figure 8. Since the latter is not accurately triangular, a condition of complete absence of oscillation could not be attained at $z = 13.1$, 17.5, and 21.8.

It would seem natural to design a cam producing no oscillations by combining, by harmonic analysis, the first 12 harmonics. This cam would produce absolutely no vibrations for $z > 12$. The straight lines of the upper and lower part of the cam would, however, according to this synthesis have to be replaced by a wave form of contour. A more promising method would be to use a range of z giving few oscillations; for example, $z = 21.8$ to 28.4 (combination of a zero point of the first kind with two zero points of the second kind). It should be noted also that the oscillation amplitudes for a sine half-wave are smaller than those for a triangular wave.

The same zero points as in figure 19 appear when a spring without mass to which a point mass is attached at the center is caused to vibrate. We are therefore justified in the assumption that a long spring with a guiding piston in the center would show the same zero points as a spring without a concentrated mass if the natural frequency f is computed according to the Dunkerley formula:

$$\frac{1}{f^2} = \frac{1}{f_m^2} + \frac{1}{f_f^2} \qquad (14)$$

f_m is the natural frequency of the concentrated mass attached to a spring assumed without mass.

f_f is the natural frequency of spring without the concentrated mass.

THE SETTING UP OF RESONANCE

If a mass that is elastically supported is suddenly acted on by a sine varying force having the same natural frequency as the mass, the latter will be set vibrating in resonance and the amplitude will continually increase until after a certain time a steady state is reached. A spring behaves in the same way. When the shaft speed is a multiple of the natural oscillation period there would be, if there were no damping, an equal increment in the oscillation amplitude for each lift. Due to internal friction in the material and air friction the amplitude between the lifts decreases. A steady state is reached when the loss per rotation due to damping is equal to the amplitude for a single lift.

The setting up of the resonance vibrations may be mathematically considered in the following way:

The amplitude of the oscillation, as will later be shown experimentally, decreases according to an exponential law, the ratio of two successive amplitudes being constant

$$\frac{A_{n+1}}{A_n} = \alpha$$

After one cam revolution, i.e., after z oscillations the amplitude ratio becomes

$$\frac{A_{n+z}}{A_n} = \alpha^z$$

The damped harmonic oscillation may be represented by a vector whose end describes a logarithmic spiral. In the case of resonance the vector, during one revolution of the cam, rotates exactly z times for every 360°. If the oscillation amplitude for a single lift is A (measured in nondimensional units τ_{dyn}/τ_o) this is superposed on the reduced amplitude of the previous lift $A\,\alpha^z$. The previous lifts contribute the amounts $A\,\alpha^{2z}$, $A\,\alpha^{3z}$, $A\,\alpha^{4z}$, etc., and their sum amounts to

$$A\,(1 + \alpha^z + \alpha^{2z} + \alpha^{3z} \ldots) = \frac{A}{1 - \alpha^z} = AR \qquad (15)$$

To obtain the amplitude of the final resonance vibra-

tion the amplitude for a single stroke A must be multiplied by the resonance factor $R = 1/1-\alpha^z$.

Figure 21 shows the resonance factor plotted for $z = 5$ to 50 and $A_n/A_{n+1} = 1.005$ to 1.10. The chart is sufficient for all practical purposes.

Between two resonance positions - i.e., for $z = a + 0.5$ (a is an integer) the phase difference of two superposed vectors is not 360° as above but $(a + 0.5)\ 360°$. Each vector therefore acts in opposition to the previous one and the "intermediate resonance factor" becomes:

$$A\ (1 - \alpha^z + \alpha^{2z} - \alpha^{3z} + \alpha^{4z} \ldots.) = \frac{A}{1 + \alpha^z}$$

$$1 > \frac{1}{1 + \alpha^z} > 0.5$$

In figure 22 the spring vibration was computed for $z = 19$. The spaces in between stand for the lift which for simplicity was not indicated. After each stroke the oscillation receives the constant increment A until the loss by damping becomes equal to A and the steady state is reached.

For $z = a + 0.5$, if there were no damping, the successive rotations would alternately give amplitudes of 2A and zero. On account of the damping, this does not occur but instead the condition shown on figure 22 for $z = 18.5$. According to the amount of the damping, a value between A and A/2 is reached in the steady state. The same applies to the building up of the oscillations for $z = a + 2/3$; for example, $z = 18-2/3$. Figure 22 should be compared with the corresponding oscillograms, figure 23. Figure 24 shows the oscillograms for the resonance positions for $z = 12$ to 23 and was obtained in the same manner as figures 16 and 17.

If the theoretically computed amplitudes for a single lift (fig. 18) are multiplied by the resonance factor obtained from figure 21, there are obtained the theoretical resonance amplitudes of figure 25, which are in satisfactory agreement with the oscillographed amplitudes of figure 24. The damping required to compute the resonance factor was determined by the experiments to be described later.

FORCED SPRING OSCILLATION WITH DAMPING

The general solution of the differential equation of damped spring oscillation is, according to Hort (reference 6):

$$y = e^{-bx} [C_1 \sin (\omega t - ax) + C_2 \cos (\omega t - ax)] +$$

$$+ e^{+bx} [C_3 \sin (\omega t + ax) + C_4 \cos (\omega t + ax)]$$

At the fixed end of the spring, let $x = 0$ and $y = 0$, whence we obtain:

$$C_1 = -C_3 \qquad C_2 = -C_4$$

Let the end of the spring $x = l$ be moved by an excentric in accordance with the law

$$(y)_{x=l} = r \sin \omega t$$

This end condition gives two more equations for determining the constants. Carrying out the computation, we obtain for the damped and forced spring oscillation, the following equation:

$$\frac{y}{r} = \frac{e^{-bx}\left\{[e^{-bl} - e^{bl}] \cos al \sin(\omega t - ax) + [e^{-bl} + e^{bl}] \sin al \cos(\omega t - ax)\right\}}{e^{-2bl} - 2 \cos 2al + e^{2bl}} -$$

$$- \frac{e^{bx}\left\{[e^{-bl} - e^{bl}] \cos al \sin(\omega t + ax) + [e^{-bl} + e^{bl}] \sin al \cos(\omega t + ax)\right\}}{e^{-2bl} - 2 \cos 2al + e^{2bl}} \qquad (16)$$

From this equation, by neglecting the damping coefficient b, there is obtained the simple relation which was first given by Fröhlich:

$$y = r \frac{\sin \omega t \sin ax}{\sin al} \qquad (17)$$

The constants a and b may be determined by substituting a part integral into the partial differential equation:

$$a = \sqrt{\frac{1}{2}\left\{\sqrt{\frac{\omega^2}{c^2}(\mu^2 \omega^2 + k^2)} + \frac{\mu}{c}\omega^2\right\}} \cong \frac{\omega}{w_s}$$

$$b = \sqrt{\frac{1}{2}\left\{\sqrt{\frac{\omega^2}{c^2}(\mu^2 \omega^2 + k^2)} - \frac{\mu}{c}\omega^2\right\}} \cong \frac{k}{2\mu} \frac{1}{w_s} \qquad (18)$$

The changes in the spring force at the fixed end of the spring are obtained by the partial differentiation of equation (16):

$$(P)_{x=o} = c \left(\frac{\partial y}{\partial x}\right)_{x=o}$$

Since we are interested only in the amplitude for the case of resonance we set in equation (16), as the condition for resonance, the approximation

$$al \cong \frac{\omega}{w_s} l = \pi$$

The result of both operations gives:

$$(P)_{x=o} = P_{dyn} = \frac{r\omega c}{w_s} \frac{2}{e^{bl} - e^{-bl}} \sin(\omega t + \psi)$$

The force for very slow motion is equal to

$$P_o = \frac{r}{l} c \sin \omega t$$

and the ratio of amplitudes is

$$\left|\frac{P_{dyn}}{P_o}\right| = \left|\frac{\tau_{dyn}}{\tau_o}\right| = \frac{\omega}{w_s} l \frac{2}{e^{bl} - e^{-bl}} = \pi \frac{2}{e^{bl} - e^{-bl}} \qquad (19)$$

From equation (9) we obtain for a single sine motion of the spring end ($z = 1$, $h = r$)

$$\frac{\tau_{dyn}}{\tau_o} = 2\pi$$

The resonance factor (for $z = 1$)

$$R = \frac{1}{1 - \left(\frac{A_{n+1}}{A_n}\right)^z} = \frac{1}{1 - \frac{A_{n+1}}{A_n}}$$

is transformed by the means of the relation:

$$2bl = 2 \frac{k}{2\mu} \frac{l}{w_s} = \frac{k}{2\mu} T_o = \ln \frac{A_n}{A_{n+1}}$$

into

$$R = \frac{1}{1 - e^{-2bl}} = \frac{e^{bl}}{e^{bl} - e^{-bl}}$$

The approximate equation then reads:

$$\frac{\tau_{dyn}}{\tau_o} = 2\pi \frac{e^{bl}}{e^{bl} - e^{-bl}} \qquad (20)$$

and differs from equation (19) only by the factor e^{bl} which, for springs that are damped by the air resistance, may be set equal to 1 to within a few percent. The difference consists in the neglecting of the damping during the lift in the case of the approximate solution.

FREE VIBRATION OF THE SPRING

The fundamental frequency for round steel springs is computed by the formula

$$f = 358{,}000 \frac{\delta}{pd^2}$$

where δ is the diameter of wire in millimeters

d, mean diameter of coil in millimeters

p, number of coils

To test the accuracy of the calculation, the natural frequencies of 10 springs of various dimensions were measured. The springs were set vibrating at their natural frequencies and an oscillogram obtained for the steadily diminishing vibrations. By comparing with the accurately calibrated sine line of the time-recording instrument, the following natural frequencies were established:

δ =	3	4	4.5	5.5	6 mm
d =	36	38	38	40	40 mm
p =	9	12.5	9.5	9	4 turns
f measured =	104	85	114	141	348/sec.
f computed =	92	79	117	137	335/sec.

δ =	6	6	6.5	7	8 mm
d =	38	42	44	43	40 mm
p =	11	14	9	7	15 turns
f measured =	135	87	152	198	119/sec.
f computed =	135	87	133	194	119.5/sec.

The deviations are such that any attempt to avoid resonance by computation beforehand is unsuccessful. The resonance speeds at a natural frequency of 6,000/minute, for example, are:

300, 316, 333, 353, 375/minute

The critical speeds lie so near each other that resonance is set up in the spring almost at any engine speed since the free oscillations of identical springs deviate slightly due to faults in manufacture. To avoid spring surges it is therefore necessary to compute only the ranges within which there occurs little vibration if there is no possibility of obtaining sufficient damping.

THE DAMPING OF SPRING OSCILLATIONS

The general differential equation for damped spring vibration according to equation (1) includes the following solution for the free oscillation:

$$y = e^{-\frac{k}{2\mu}t} \sum_{\nu=1}^{\nu=\infty} \left\{ \left[A_\nu \sin \omega_\nu t + B_\nu \cos \omega_\nu t \right] \sin \frac{\nu\pi}{e} x + \left[C_\nu \sin \omega_\nu t + D_\nu \cos \omega_\nu t \right] \cos \frac{\nu\pi}{l} x \right\}$$

where $\omega_\nu = \sqrt{\nu^2 \omega_o^2 - \left(\frac{k}{2\mu}\right)^2}$ $\omega_o = \frac{w_{\text{ft}}}{l} \pi$

According to the mode of excitation, the dying-down vibration may be considered as made up of standing waves of various orders. The period changes very little with the order. Example:

Example: $\omega_0 \cong 1200$; $k/2\mu \cong 5$

$\omega_1 = 0.9992\ \omega_0$; $\omega_\infty = 1.000\ \omega_0$

After a completed fundamental vibration, there is set up between the fundamental and a higher harmonic a phase shift of at most 0.3°. The form of the curve therefore changes little during the dying down of the oscillation as Frohlich has shown in a simple experiment.

The form of the solution likewise shows, however, that the amplitudes, and therefore also the stresses at the spring end, decrease at the same rate in the same time interval for all orders according to the amount contributed by the quotient $k/2\mu$. The reduced mass per centimeter of wire μ depends only on the wire diameter and on the specific weight, and k is a function only of the wire diameter. It is therefore to be expected that $k/2\mu$ is likewise dependent only on the wire diameter. In order to test this assumption, the damping of the oscillograms which were used to determine the frequency was evaluated. In obtaining the damped curves the sensitivity of the indicator was so adjusted that the vibrations died down in the same manner as those of spring vibrations. The oscillogram of such a vibration (fig. 26) reveals vibration phenomena of a type that could not be entirely explained. It was at first thought that they were vibrations transverse to the spring axis. Similar phenomena were revealed to a slighter extent in the case of the other springs.

Figure 27 shows the logarithms of the amplitudes plotted against the oscillation number for several springs. A straight line was drawn through the scattered points. (The series of points forming a wave belongs to the oscillogram (fig. 26).) The inclination of the straight lines determines the value of the damping. The magnitude

$$\frac{k}{2\mu} = f \ln \frac{A_n}{A_{n+1}}$$

plotted against the wire diameter (fig. 28) shows that the former is affected by still another factor. It was particularly observed that in the case of four springs having equal wire diameter and approximately equal diameter of coils, the damping was smaller the longer the spring. The values for the damping were:

No. of turns	p = 4	11	14	17	$\delta = 6$; $d \cong 40$ mm
	$k/2\mu$ = 7.2	3.3	1.45	0.58	

This effect can only be explained as due to the additional damping at the end of the spring, which we may denote as the loss due to reflection, and which is composed of the following components:

1. Friction of the spring wire at the spring end.

2. Friction between the spring coils during the unwinding of the last coil.

3. Dissipation of sound energy from the spring end to the engine mass.

That reflection losses which cannot be taken into account by computation occur, could be confirmed by the following test:

The same spring ($\delta = 6$; $d = 40$; $p = 17$) under identical conditions was successively supported on leather, rubber, and "polyperite," and investigated for damping. The supports consisted of rings of 5 millimeters thickness and of the same inside and outside diameter as the spring. The rings were inserted at each end between the spring and the spring washer. Figure 29 shows the oscillograms obtained, the initial amplitude being the same in each case. (The softer the support, the greater the loss by reflection.) Considerable damping may be attained by pressing sheet-metal tongues against the spring, and the damping could be adjusted by the amount of pressure applied. In figure 30a, for example, the vibration dies down completely during one rotation; 30b was obtained with the spring in lubricating oil. With cylinder oil no oscillations could be observed between $z = 12$ and 24. In order to render the magnitude of the damping visible, the spring was slackened to such an extent that it began to knock against the follower and started a vibration (fig. 30c).

EFFECT OF INITIAL SPRING TENSION

In accordance with the theory developed, the amplitudes of the resonance vibrations should be independent of the initial spring tension. Swan and Savage found, however, an increase in the amplitude with increasing initial tension. The author has, therefore, for $z = 20$, varied the initial tension from the knocking spring condition until the condition where the coils almost touched (fig. 31).

The average play between the turns at the upper cam position was chosen as parameter (fig. 31c). The natural vibrations increase somewhat with increasing initial tension in agreement with the results of Swan and Savage, since the spring becomes somewhat shorter by the compression of the spring end (fig. 31b).

At a play of 3 millimeters the roller begins to knock and for this reason the spring is damped somewhat. As the play becomes smaller the amplitude diminishes almost inappreciably while there is a strong decrease between 1 and 0.33 millimeter. The damping here increases because the spring coils at the upper cam position touch each other. A shrill sound is emitted whereas for a smaller initial tension a deeper hum corresponding to the natural frequency is heard.

EFFECT OF PLAY BETWEEN CAM AND FOLLOWER

Swan and Savage found a strong variation of the vibration frequencies with the amount of follower play. This is to be expected since the velocity of the spring end varies with the amount of play of the roller. Swan and Savage increased the amount of the play up to 1.5 millimeters for a lift of about 9 millimeters. In the present set-up the lift was 18 millimeters, and for a play of the roller of 0.8 millimeter, the knocking was so strong that no increase in the play was possible. Within this limiting value diagrams were obtained for four different plays for a single lift and compared with the theoretical one ($z = 20$). The comparison shows that the amplitude for a play of 0 to 0.8 millimeter between cam and follower does not appreciably vary (fig. 32).

When the vibrations are few, for example, $z = 17$, the conditions are different. In this case a certain velocity is suddenly set up at the beginning and end of the velocity curve where a small triangle is cut off. With these triangles superposed according to equation (9), there is obtained an oscillation diagram showing a large number of sharp points (fig. 33). There was no agreement, however, with the oscillogram since the shocks due to the strokes were transmitted to the quartz crystal and covered up the details on the oscillogram.

Assuming the camshaft to be accelerated to a constant rotational velocity before the first lift stroke begins, then at the start of the first stroke the tension increases linearly with the velocity of the spring end up to the return of the disturbance which is reflected at the fixed end of the spring. The succeeding stresses are the result of the superposition of all the disturbance waves that run up and back and oscillate about a mean line that increases linearly with the lift.

After the first lift there remains behind an oscillation which, for example, for 10 natural vibrations per rotation, contains the 10th, 20th, 30th, etc. harmonics of the velocity curve. The amplitude of the vibration is more easily computed with the aid of superposition than by means of harmonic analysis. The magnitude of the vibration excited after the first lift as a function of the number of vibrations per turn indicates to the designer in what range of engine speeds particularly large resonance frequencies are set up. It is shown by means of an example how a sufficiently large range of rotational speeds may be obtained within which little vibration occurs.

If the natural frequency is an exact multiple of the cam speed the vibration amplitude will increase by the same amount after each stroke. As a result of the damping, however, a steady state will be reached as soon as the increase per rotation has become equal to the loss by damping. In a set of curves a resonance factor is given by which the computed amplitude of the first lift must be multiplied in order to obtain the final steady amplitude. This resonance factor changes with the amount of the damping and with the number of oscillations per rotation.

The damping depends not only on the air resistance and on the internal friction of the material but also on the manner in which the spring is supported (loss by reflection). In lubricating oil the damping is so large that the vibrations die down before the next lift stroke.

The phenomena described were confirmed by numerous tests with cams and springs. Oscillograph measurements of the forces at the spring ends show satisfactory agreement with the curves computed beforehand.

The present work was carried out at spare intervals at the physics laboratory of the firm of Sulzer Brothers, Winterthur. The firm kindly placed at my disposal the

spring test apparatus, the Siemens Universal oscillographs, and the quartz indicators, for which I here take the opportunity to express my sincere thanks.

I wish to thank Professor Eichelberg, who submitted my report, for the kind interest he has shown throughout my investigations.

Translation by S. Reiss,
National Advisory Committee
for Aeronautics.

REFERENCES

1. Weibull, W.: De dynamiska agenskaperna bos spiralfjädrar, Stockholm, 1927.

2. Savage: The Surging of Engine-Valve Springs. Engineering Research, special report No. 10. His Majesty's Stationery Office, London, 1928.

3. von Lehr: Z. d. V. D. I., 1933, p. 458.

4. Kluge, J., and Linckh, H. E.: Forschung auf dem Gebiete des Ingenieurwesens, May 1931, p. 153.

5. Fröhlich: Z. f. Mathematik und Physik, 1908, p. 379. Magg. Verh. d. Ver. z. Beförd. d. Gewerbefleisses, 1912, p. 480.

6. Hort: Die Differentialgleichungen des Ingenieurs, 1925, p. 585.

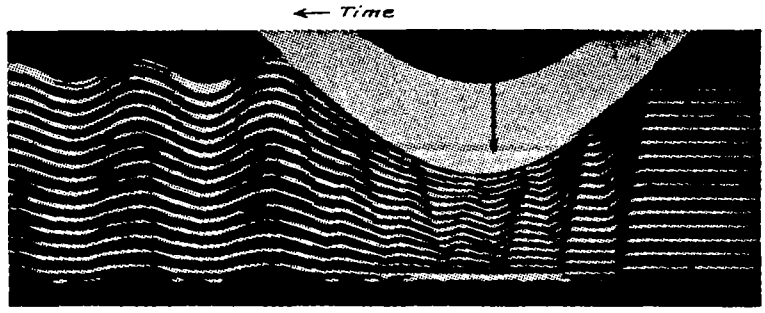

Figure 1.- Multiple reflection of a disturbance at a spring.

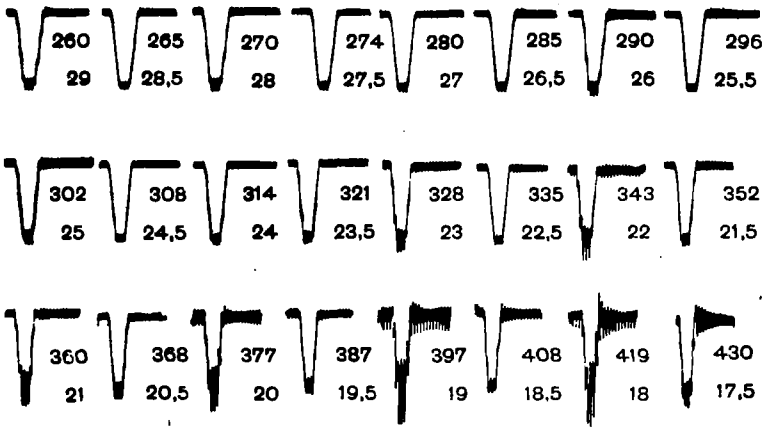

Figure 5.- Resonance frequencies of spring with natural frequency of 7540/min. Nos. 260 to 430 indicated rotations per minute. Nos. 29 to 17.5 indicate number of free oscillations per rotation.

Figure 4.- Section through the test apparatus, a = test spring.

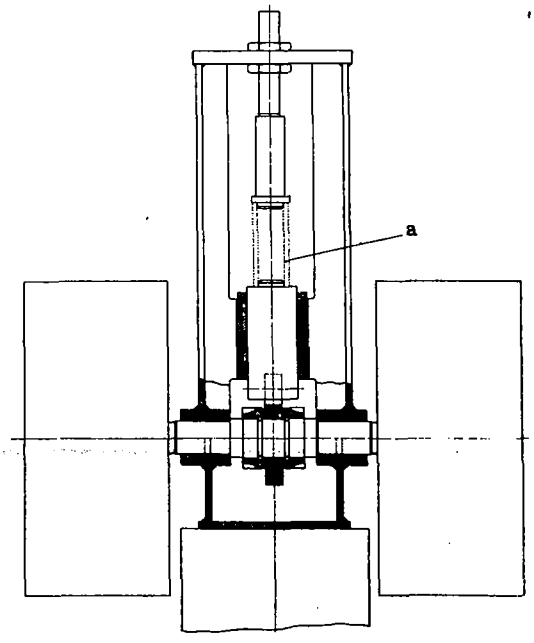

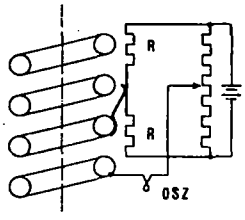

Figure 2.- Sketch showing recording of vibration by means of a bridge.

Figure 3.- Motion of the center spring coil obtained with the apparatus of fig.2.

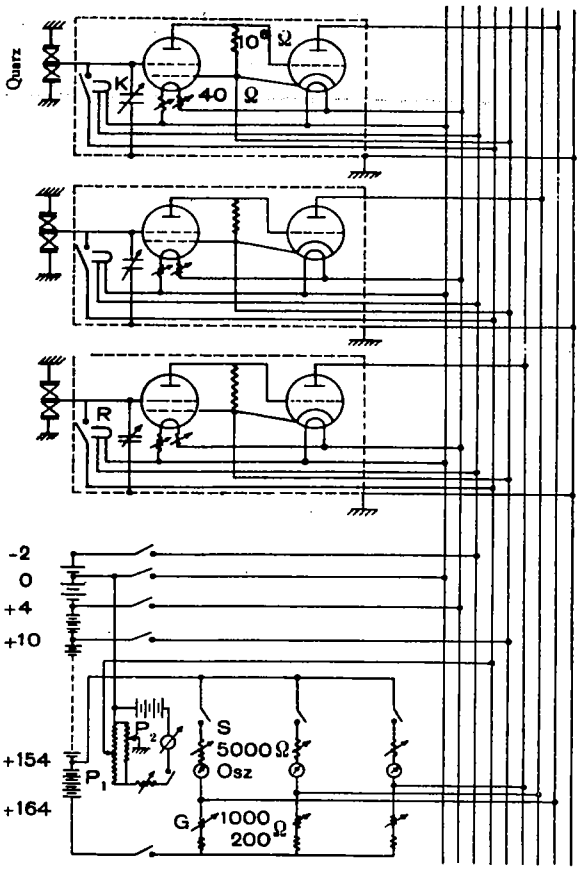

Figure 6.- Scheme of connections of amplifier.

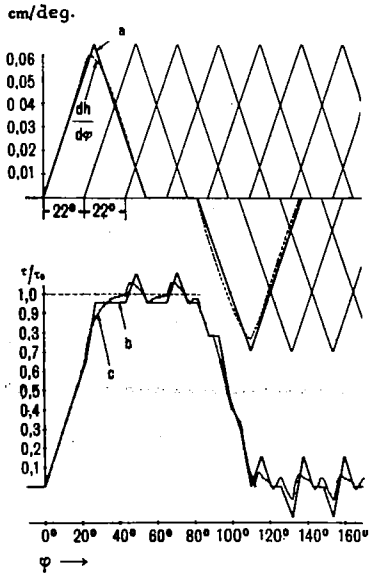

Fig.9

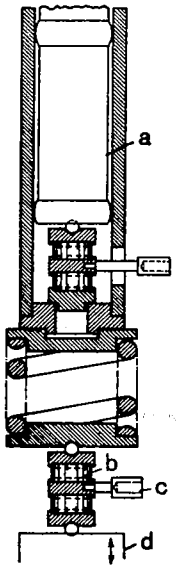

Fig.10

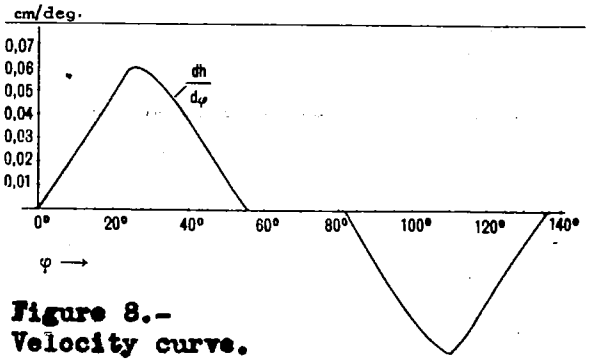

Figure 8.- Velocity curve.

Figure 11.- Computed stress curve.
a, at the stationary end of the spring.
b, at the moving end of the spring.

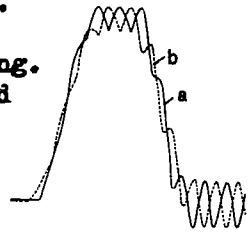

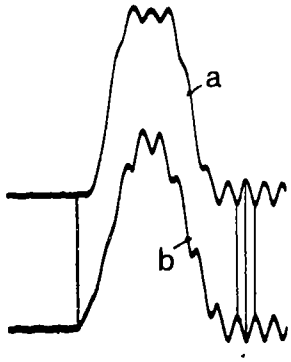

Figure 12.- Oscillographs of stresses of fig.11.
a, at stationary end of spring.
b, at moving end of spring.

Figure 9.- Stress variation for a single lift for z = 16.4.
a, Curve to replace the exact dh/dφ curve.
b, Stress computed from curve a.
c, Stress computed from exact curve.

Figure 10.- Section through spring with quartz indicator.
a, rigid support.
b, quartz crystal.
c, electrode to amplifier.
d, moveable guide.

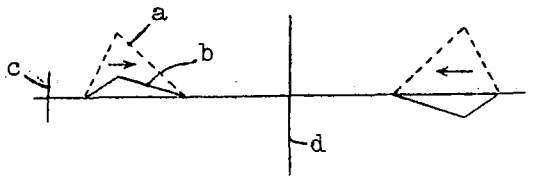

Figure 7.- Reflection of disturbance at a fixed wall.
a = stress. c = moving end of spring.
b = velocity. d = reflecting wall.

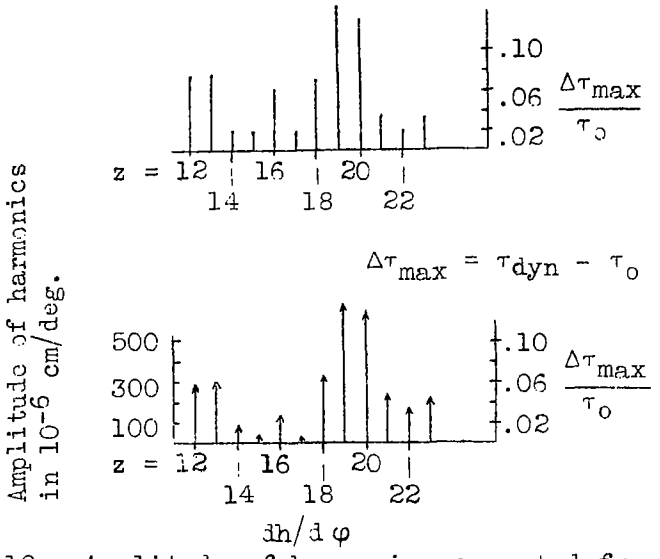

Figure 18.- Amplitude of harmonics computed from the wave theory and compared with the results of harmonic analysis.

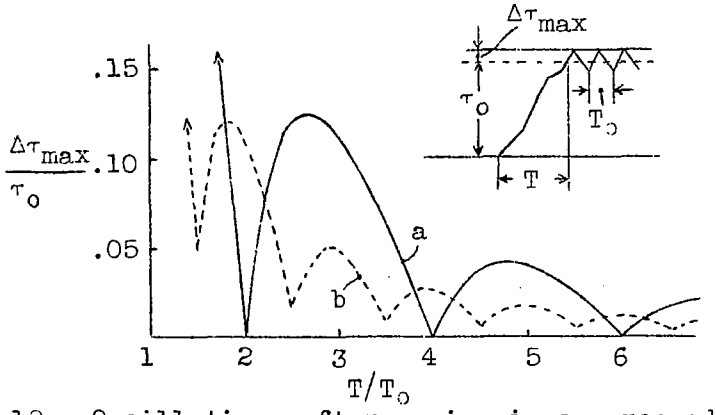

Figure 19.- Oscillations after spring is compressed, then released. a = with triangular form of velocity curve. b = with velocity curve in form of half sine wave.

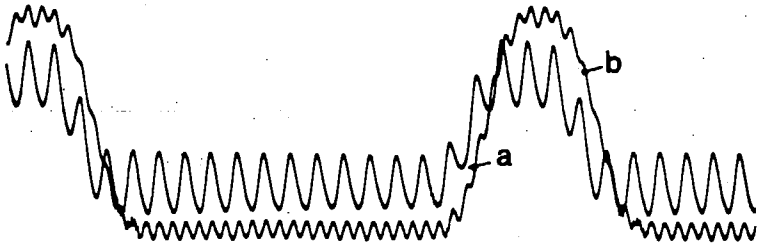

Figure 14.- a, proof of the existence of the second (more accurately even) harmonics by adding electrically the forces at the spring ends.
b, comparison with the forces at the stationary end (z = 19).
Both curves were obtained one directly after the other.

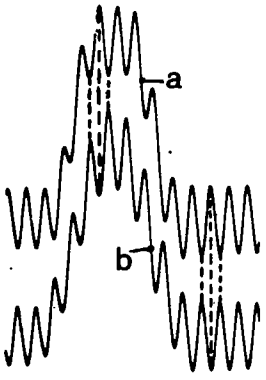

Figure 13.- Spring stresses at both ends of the spring synchronously recorded (z = 20).
a, stationary end.
b, moving end.

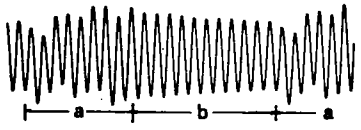

Figure 15.- Difference of end pressures
a, building up again of damped oscillations during the lift stroke.
b, dying down during down motion of the cam.

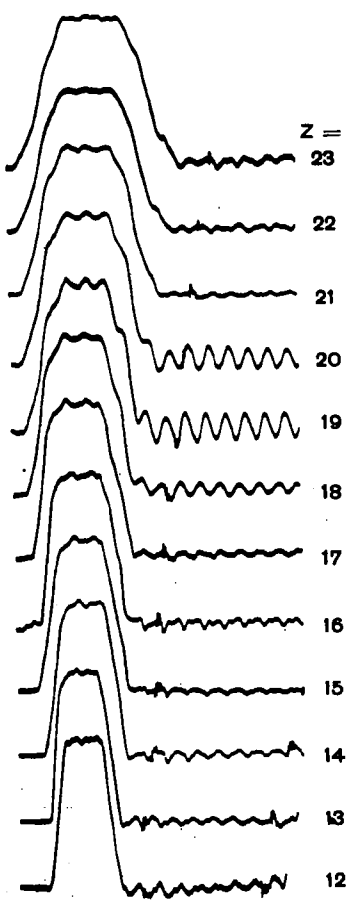

Figure 16.- Oscillograms for single lift.

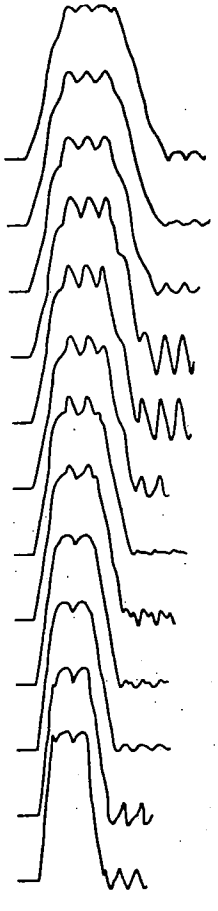

Figure 17.- Same curves computed.

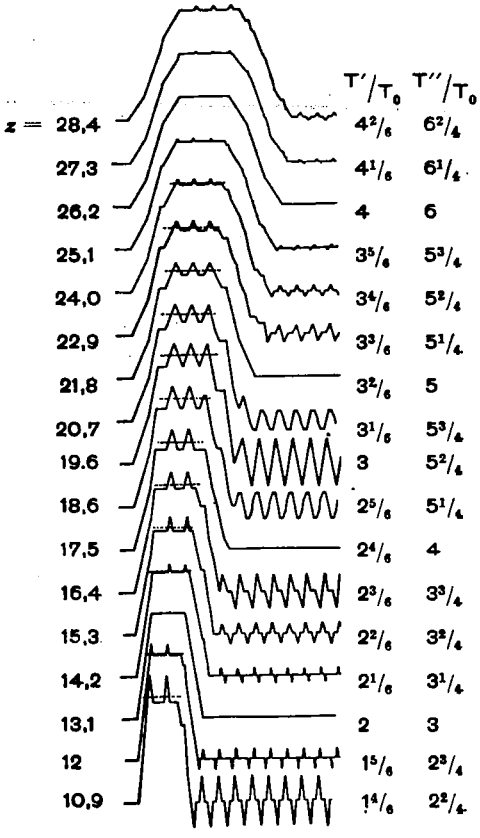

Figure 20.- Computed stress curves for a triangular velocity curve.

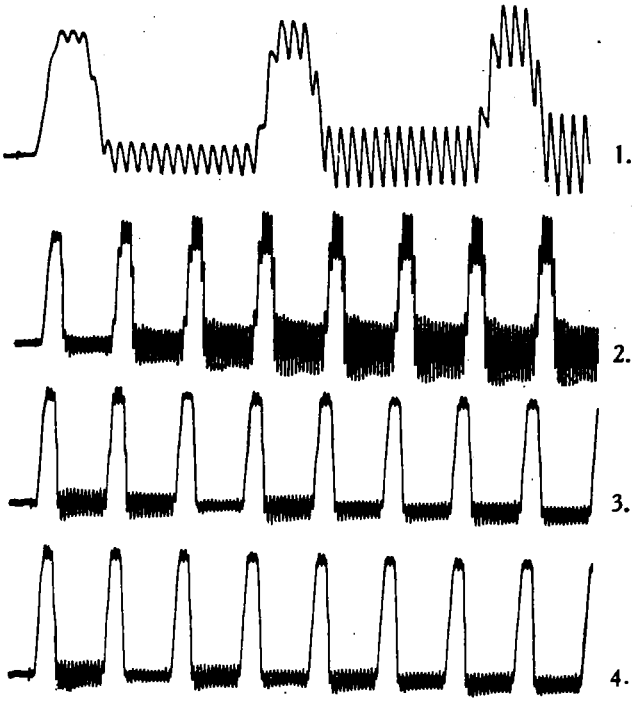

Figure 23.- Building up spring vibrations, obtained with oscillograph. Nos. 1 and 2: z = 19
3: z = 18 2/3
4: z = 18 1/2

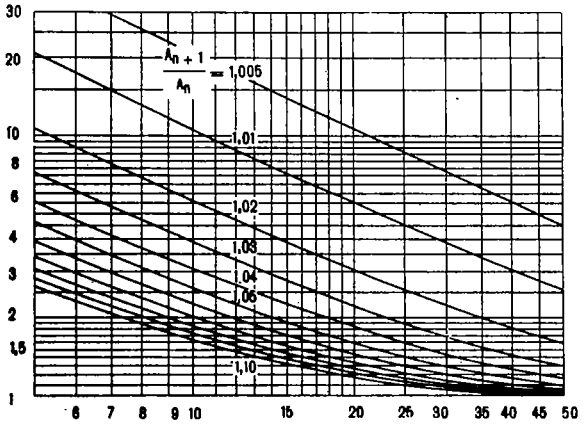

Figure 21.- Resonance factor for different numbers of oscillations per rotation.

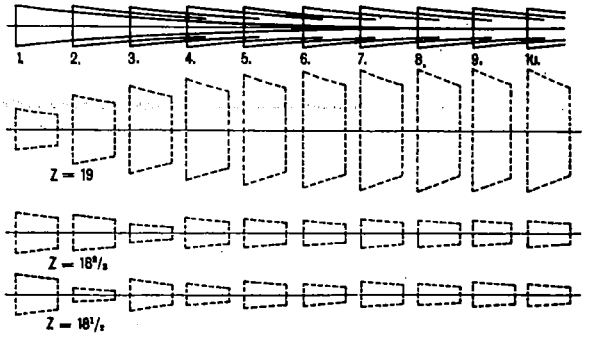

Figure 22.- Building up spring vibrations after the first lift (computed).

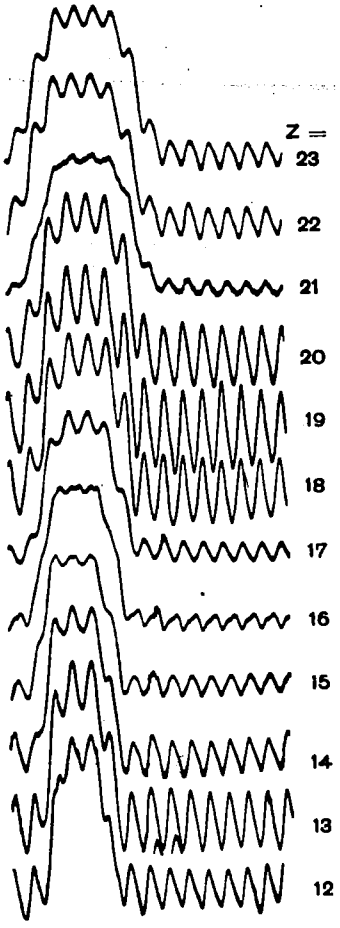

Figure 24.- Oscillograms for resonance conditions.

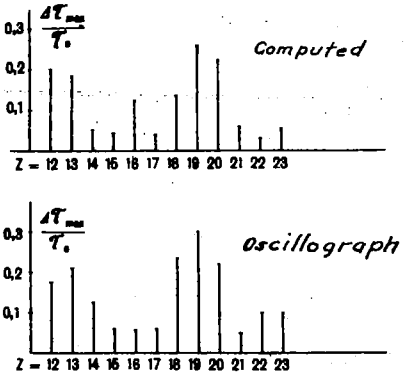

Figure 25.- Resonance amplitudes as computed and as obtained with oscillograph.

Figure 26.- Dying down of spring vibration.

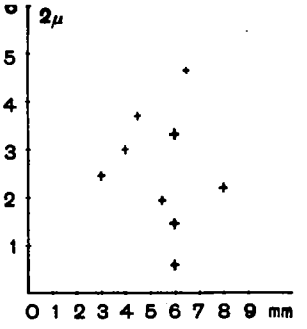

Figure 28.- Damping of tested springs as functions of wire diameter.

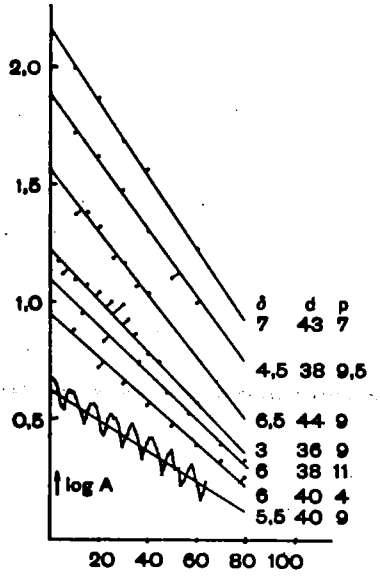

Figure 27.- Graphical determination of damping.

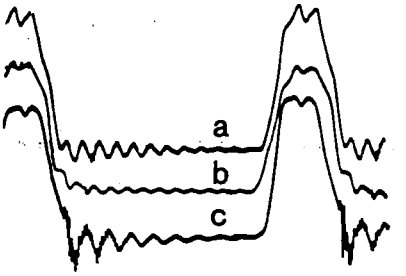

Figure 30.- Spring vibration with strong damping.

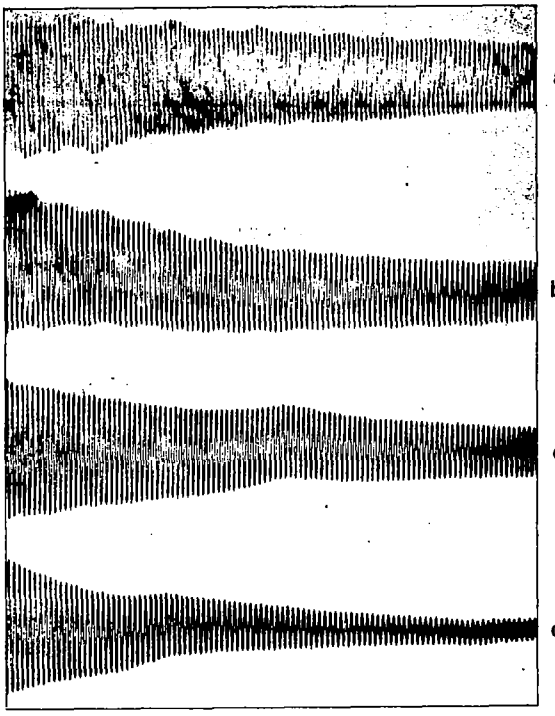

Figure 29.- Effect of yielding supports on damping.
a, without any support. c, leather ring.
b, polyperite ring. d, rubber ring.

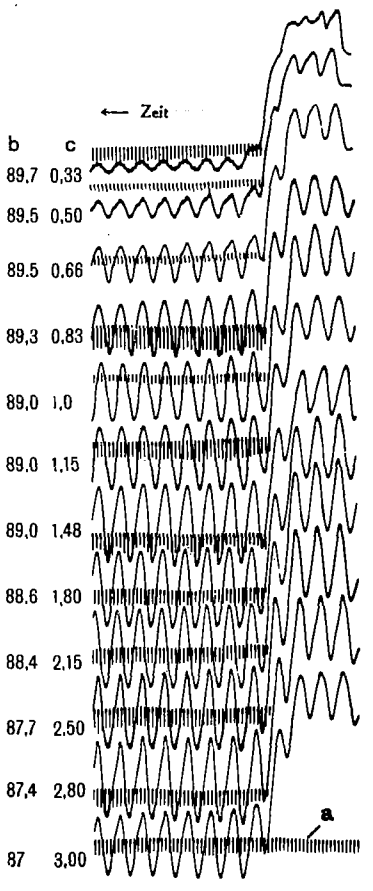

Figure 31.- Effect of initial tension: a, comparison frequency= 500/sec. b, natural spring frequency per sec. c, play between coils in mm.

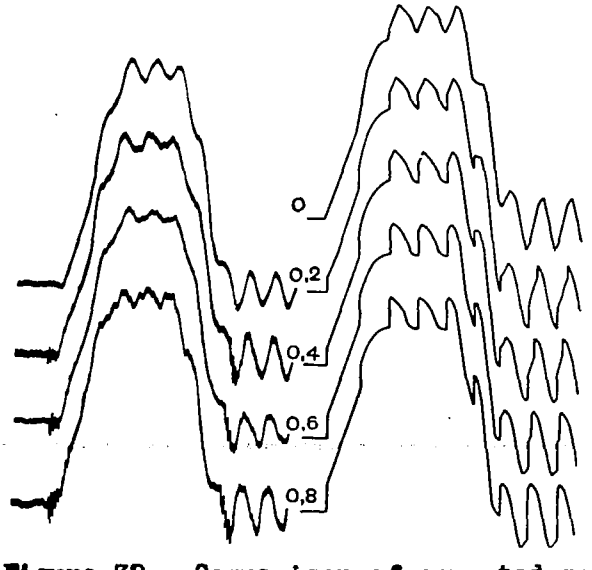

Figure 32.- Comparison of computed spring forces with oscillograms with play of roller varying between 0 and 0.8 mm. (z = 20).

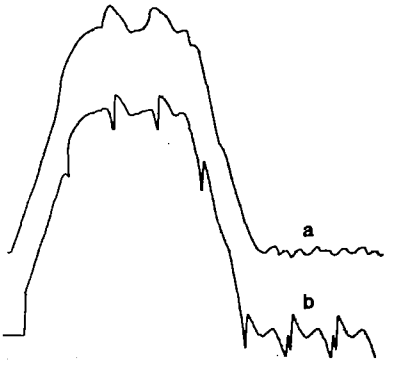

Figure 33.- Increase of oscillation amplitude due to play of roller;
a, without play.
b, with 0.8 mm. play (z = 17).